

# Scanning Tunneling Spectroscopy of Metal Phthalocyanines on a Au(111) Surface with a Ni Tip \*

JIA Zhi-Chun(贾志春), HU Zhen-Peng(胡振芃), ZHAO Ai-Di(赵爱迪), LI Zhen-Yu(李震宇), LI Bin(李斌)\*\*

Hefei National Laboratory for Physical Sciences at Microscale, University of Science and Technology of China, Hefei 230026

(Received 16 December 2010)

Scanning tunneling spectroscopy of metal phthalocyanines (MPc) adsorbed on a Au(111) surface with a Ni(111) scanning tunneling microscopy tip is simulated on the basis of first-principles calculations and a modified Bardeen approximation. Local *d* orbital symmetry matching between the molecule and the Ni tip brings obvious negative differential resistance (NDR) phenomena, of which, bias voltage and resonant orbitals can be tuned sensitively by the central ion of the molecule. Different dependences of the NDR peak on the tip-molecule distance at two bias polarities and rectifying phenomena are also interpreted in terms of specific structures of 3*d* orbitals of the adsorbed MPc and Ni tip.

PACS: 68.37.Ef, 85.65.+h, 73.63.-b

DOI:10.1088/0256-307X/28/7/076802

Molecular engineering has attracted much interest in recent years due to its huge potential in future industries such as nano-based techniques and single molecule chemistry. Scanning tunneling microscopy (STM) is a powerful tool to explore and realize molecular engineering, and has a specific experimental configuration in which a single molecule can be elaborately characterized and controlled by an STM tip. In fact, the STM technique has been employed to successfully construct prototypes of some molecular devices with typical functions such as negative differential resistance (NDR)<sup>[1]</sup> and rectification<sup>[2]</sup> effects. The STM tip is an electrode of STM configuration, so its situation is very important to the tunneling current and related properties of nano-electronics. From the last decade of the 20th century, STM tips with specific materials/components and related electronic structures have been designed and applied to realize some functions, including characterizing molecular configuration,<sup>[3]</sup> distinguishing different molecules<sup>[4]</sup> and designing molecule-based NDR devices.<sup>[5]</sup>

Recently, Chen *et al.* observed a clear NDR phenomenon when they positioned a Ni(111) tip upon the Co ion in a Co phthalocyanine (CoPc) molecule adsorbed on a Au(111) surface, and a new mechanism of local orbital symmetry matching between the Co ion and the Ni tip was proposed to interpret it.<sup>[5]</sup> Early studies have shown that the structure of the frontier orbitals of a MPc molecule can be modulated by changing the central ion in the molecule.<sup>[6]</sup> In addition, STM observations of various MPc molecules adsorbed on a metal surface presented abundant characteristics of the images and spectroscopy of molecules, which are closely related to the central metal ion.<sup>[7–10]</sup> Thus one will expect that different MPc molecules with different central metal ions can couple with a Ni tip, which has been proved to possess specific electronic structures of

*d* orbitals, to provide more characteristics of scanning tunneling spectroscopy (STS). In this Letter, we employ the first-principles calculations based on density functional theory (DFT) and the modified Bardeen approximation (MBA) to simulate the STS of various 3*d* transition metal MPc (M = Mn, Fe, Ni, and Cu) molecules adsorbed on a Au(111) surface when using a Ni(111) STM tip, and to explore how different metal ions influence the main characteristics of STS in this STM configuration, which may be applied in future molecular electronics, especially the NDR phenomena.

The electronic structures of the MPc molecules adsorbed on a Au surface and the Ni(111) tip were calculated using the DFT. The Au(111) substrate was described by a slab model containing 3 layers with 56 gold atoms per layer and 7 vacuum layers, which should be large enough to eliminate slab-slab interaction. The MPc molecules were placed parallel to the Au(111) surface<sup>[11]</sup> with the most stable configuration deduced in Ref. [9] (Figs. 1(a) and 1(b)). For the tip, we used a model of a Ni(111) surface consisting of a (3 × 3) supercell with 5 atomic layers plus a four-atom pyramid cluster (Fig. 1(c)). All calculations were carried out using the DMOL 3 package<sup>[12]</sup> in the local spin density approximation (LSDA) with the Vosko–Wilk–Nusair local correlation functional<sup>[13]</sup> and the density functional semicore pseudopotential generated by fitting the all-electron relativistic DFT results was used. The basis set consists of double-numerical atomic orbitals augmented by polarization functions. The STS was simulated with the MBA:<sup>[14]</sup>

$$I = \frac{2\pi e}{\hbar} \sum_{ts} [f(\varepsilon_t) - f(\varepsilon_s)] |M_{st}|^2 \delta(\varepsilon_t - \varepsilon_s + eV), \quad (1)$$

where  $f(\varepsilon)$  is the Fermi distribution function,  $V$  is the sample bias voltage, the energies  $\varepsilon_t$  and  $\varepsilon_s$  are relative

\*Supported by the National Natural Science Foundation of China under Grant Nos 90921013, 10704069, 20703041 and 20933006, and the Fundamental Research Funds for the Central Universities.

\*\*Correspondence author. Email: libin@mail.ustc.edu.cn

© 2011 Chinese Physical Society and IOP Publishing Ltd

to the Fermi energies  $E_F$  of the tip and sample,  $M_{st}$  is Bardeen tunneling matrix element between state  $\varphi_t$  (with energy  $\varepsilon_t$ ) of the tip and state  $\varphi_s$  ( $\varepsilon_s$ ) of the sample, i.e.

$$M_{st} = -\frac{\hbar^2}{2m} \int_{\Sigma} \varphi_t^* \nabla \varphi_s - \varphi_s \nabla \varphi_t^* dS, \quad (2)$$

where  $\Sigma$  represents any surface located in the vacuum region between both electrodes. Here, spin-polarized tunneling is not considered due to the random magnetization direction of the central ion of MPc on the Au(111) surface.

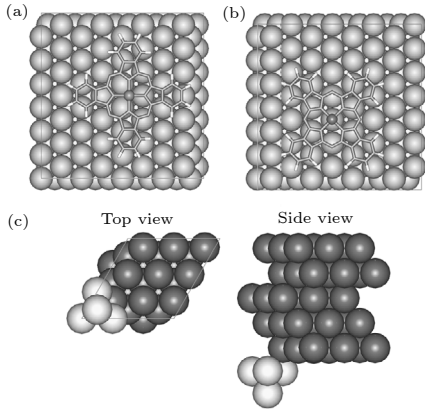


**Fig. 1.** Models of MPc ( $M = \text{Fe}, \text{Ni}$  and  $\text{Cu}$ ) (a) and MnPc (b) molecules adsorbed on the Au(111) surface, and the Ni(111) tip (c) for our simulations. The light lines indicate borderlines of one unit cell in the  $xy$  plane.

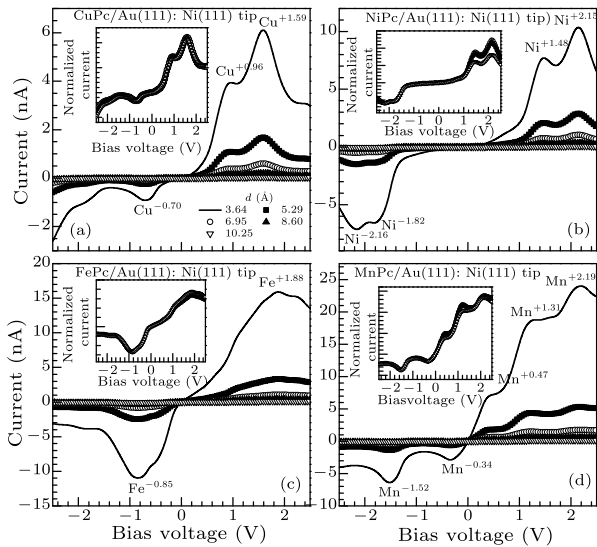


**Fig. 2.** Simulated STS curves for four MPc molecules adsorbed on the Au(111) surface with a Ni(111) tip positioned upon the central metal atoms of MPc at different tip-molecule distances. The inserts display the STS data normalized by the current at  $-1.0$  V.

Figure 2 shows our calculated STS of the optimized structures for four MPc molecules adsorbed on the Au(111) layers with a Ni(111) tip positioned upon the central metal atoms of MPc. Apparently, the NDR effect appears in all four molecules at negative and positive bias voltages, for various tip-molecule distances

$d$ . In the case of CuPc (Fig. 2(a)), the NDR effect occurs in three points (labeled as  $\text{Cu}^{-0.70}$ ,  $\text{Cu}^{+0.96}$  and  $\text{Cu}^{+1.59}$  in Fig. 2(a)), with a maximum current ( $I_{\max}$ ) at  $-0.70$  V (labeled as  $\text{Cu}^{-0.70}$ ) and a minimum current ( $I_{\min}$ ) at  $-1.37$  V, an  $I_{\max}$  at  $0.96$  V (labeled as  $\text{Cu}^{+0.96}$ ) and an  $I_{\min}$  at  $1.07$  V, and a sharp decrease in the current when the bias voltage is beyond  $1.59$  V (labeled as  $\text{Cu}^{+1.59}$ ). The NDR phenomenon at the point  $\text{Cu}^{+0.96}$  is weak because of its adjacent NDR peak  $\text{Cu}^{+1.59}$  with very strong intensity. In the case of NiPc (Fig. 2(b)), the NDR points are labeled as  $\text{Ni}^{-2.16}$ ,  $\text{Ni}^{-1.82}$ ,  $\text{Ni}^{+1.48}$  and  $\text{Ni}^{+2.15}$  but the former two are so adjacent that a broad NDR peak appears. In the case of FePc (Fig. 2(c)), it seems that there are two obvious NDR peaks ( $\text{Fe}^{-0.85}$  and  $\text{Fe}^{+1.88}$ ) appearing at negative and positive biases, respectively, but careful checking will find that both are composed of multiple NDR peaks with similar intensities. The most complex STS occurs in the case of MnPc (Fig. 2(d)): the NDR phenomena occur at five different points  $\text{Mn}^{-1.52}$ ,  $\text{Mn}^{-0.34}$ ,  $\text{Mn}^{+0.47}$ ,  $\text{Mn}^{+1.31}$  and  $\text{Mn}^{+2.19}$ , although the three ones at positive bias are weaker, especially  $\text{Mn}^{+0.47}$  and  $\text{Mn}^{+1.31}$ , resembling a “shoulder” at some tip-molecule distances. The normalized STS by the current at  $-1.0$  V are also calculated to check the influence of the tip-molecule distance on the STS. The results show that main properties of the STS, especially the NDR phenomena, remain unchanged on the whole, but in the cases of NiPc, FePc and MnPc, variations of the intensities of the NDR peaks with enlarged tip-molecule distance  $d$  are different at negative and positive biases.

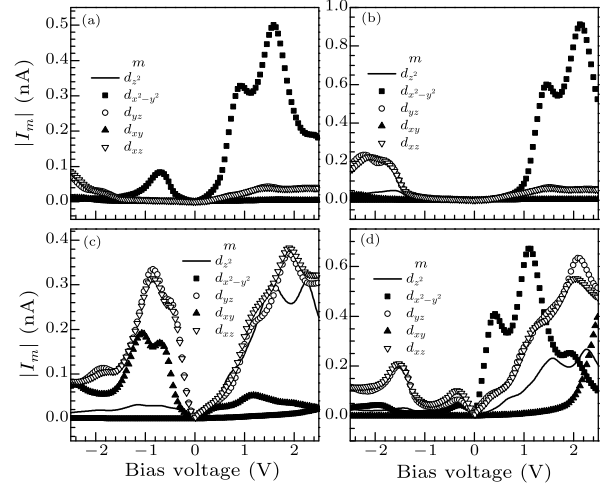


**Fig. 3.** Simulated partial tunneling currents  $|I_m|$  versus bias voltage contributed from five  $3d$  orbital components of the central metal atom in the adsorbed MPc molecule and the terminal Ni atom in the Ni(111) tip: (a)  $M = \text{Cu}$ , (b)  $M = \text{Ni}$ , (c)  $M = \text{Fe}$ , (d)  $M = \text{Mn}$ .

To explain the above-mentioned NDR effects, we have calculated the partial tunneling currents  $I_m$  contributed from five  $3d$  orbital components ( $m = d_{z^2}$ ,  $d_{x^2-y^2}$ ,  $d_{yz}$ ,  $d_{xy}$  and  $d_{xz}$ , and  $s$  and  $p$  orbitals contribute much less according to our calculations) of the central metal atom in the adsorbed MPc molecule and

the terminal Ni atom in the Ni(111) tip, which dominate the total currents, using the new form of the MBA proposed in Ref. [5]. The  $|I_m|$ - $V$  characteristics for four cases are shown in Fig. 3, with the tip-molecule distance of 6.95 Å. Their behaviors can be easily understood with the help of the partial density of states (PDOS) of the MPc molecule and the Ni(111) tip (Fig. 4), based on the mechanism of local orbital symmetry matching.<sup>[5]</sup>

In the case of CuPc, the PDOS of Cu ion is dominated by  $d_{x^2-y^2}$  orbital at  $-0.52$  eV and  $+0.62$  eV relative to the  $E_F$  (Fig. 4(a)), and this orbital also has obvious contributions in the PDOS of the Ni atom on the tip at  $-0.98$  eV,  $-0.27$  eV and  $+0.21$  eV relative to the  $E_F$  (Fig. 4(e)) (almost overlapping the PDOS of  $d_{xy}$ ). Figure 3(a) shows that the  $d_{x^2-y^2}$  orbital forms dominant channels for the electron tunneling and is responsible for three NDR in the STS. Thus we can deduce that the NDR occurring at  $-0.70$  V ( $\text{Cu}^{-0.70}$ ) could be contributing to the resonant tunneling between the  $d_{x^2-y^2}$  at  $-0.52$  eV in Cu and the tiny peak of the same orbital at  $+0.21$  eV in the Ni tip, and  $\text{Cu}^{+0.96}$  and  $\text{Cu}^{+1.59}$  are formed by the resonant tunneling between the  $d_{x^2-y^2}$  at  $+0.62$  eV in Cu and the two peaks ( $-0.27$  eV,  $-0.98$  eV) in the Ni tip, respectively. Although some of the other  $d$  orbitals have relatively large contributions to the PDOS of the Ni atom, their fewer contributions to the PDOS of Cu near the  $E_F$  results in smaller tunneling currents from them.

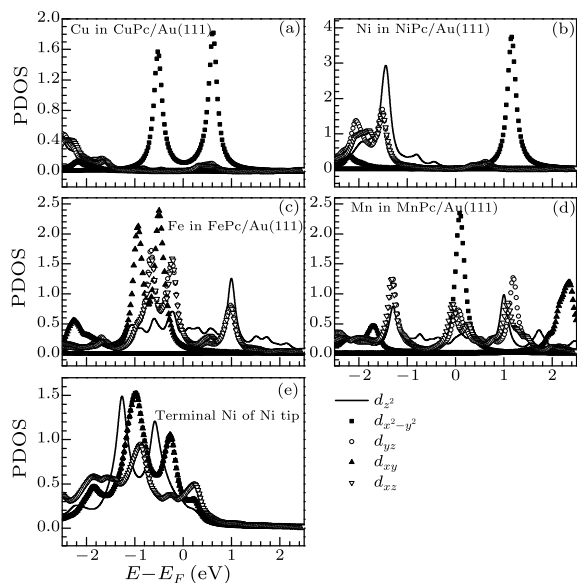


**Fig. 4.** PDOS of the central metal atom in the MPc molecule ((a)–(d)) and the terminal Ni atom in the Ni(111) tip (e). One should note degenerate PDOS of  $d_{x^2-y^2}$  and  $d_{xy}$ , and that of  $d_{xz}$  and  $d_{yz}$  in (e).

For the case of NiPc, the STS has two NDR points at each bias polarity. The partial currents contributed from five  $d$  orbital components are shown in Fig. 3(b). It is evident that the NDR occurring at  $+1.48$  V ( $\text{Ni}^{+1.48}$ ) and  $2.15$  V ( $\text{Ni}^{+2.15}$ ) are contributed from the  $d_{x^2-y^2}$  orbitals. From the PDOS of Ni tip

(Fig. 4(e)) and Ni ion in sample (Fig. 4(b)), we can deduce that the resonance tunneling between the PDOS peak of  $d_{x^2-y^2}$  at  $+1.16$  eV in the sample and the two peaks of the same orbital in tip at  $-0.27$  eV and  $-0.98$  eV results in the two NDR at positive bias. On the other hand, the NDR occurring at  $-2.25$  V and  $-1.82$  V ( $\text{Ni}^{-2.16}$  and  $\text{Ni}^{-1.82}$ ) are mainly attributed to the resonance tunneling between the  $d_{yz}$  orbitals of the sample at  $-2.06$  eV,  $-1.52$  eV and the tip at  $+0.23$  eV, intermixed with a weaker resonance tunneling between the  $d_{xz}$  orbitals weakening the NDR at  $-1.82$  V. The  $d_{z^2}$  orbital has a relatively large contribution in the DOS of the Ni atom at  $-1.44$  eV, but a lesser contribution in the PDOS of the Ni tip above the  $E_F$ , which results in a small current flowing through this channel.

In the case of FePc, although there is only one obvious NDR point in the total current at each bias polarity (Fig. 2(c)), the actual situation of the partial currents contributed from five  $3d$  orbitals is complex (Fig. 3(c)). In fact, the NDR at  $-0.85$  V ( $\text{Fe}^{-0.85}$ ) is formed jointly by the resonant tunnelings of three orbitals:  $d_{xz}$ ,  $d_{yz}$ , and  $d_{xy}$ , especially the resonant tunneling between the  $d_{xz}(d_{yz})$  orbitals of the Fe ion at  $-0.65$  ( $-0.66$ ) eV (Fig. 4(c)) and the tip at  $+0.24$  ( $+0.23$ ) eV (Fig. 4(e)), similar to the situation in the case of CoPc.<sup>[5]</sup> While at positive bias, the NDR point formed by the resonant tunneling of  $d_{xz}(d_{yz})$  orbitals crashes two NDR points formed by  $d_{z^2}$ , so there is only a weak NDR ( $\text{Fe}^{+1.88}$ ).

In the case of MnPc, the situations of both the STS and partial currents (Fig. 3(d)) are complex. The two NDR points  $\text{Mn}^{-1.52}$  and  $\text{Mn}^{-0.34}$  at negative bias still originate mainly from the resonant tunneling of  $d_{xz}(d_{yz})$  orbitals. The three NDR points at positive bias are divided into two types: the former ones ( $\text{Mn}^{+0.47}$  and  $\text{Mn}^{+1.31}$ ) are from the resonant tunneling of  $d_{x^2-y^2}$  orbitals markedly weakened by rapid increase of partial currents from the  $d_{xz}(d_{yz})$  orbitals in the same energy region; the last one ( $\text{Mn}^{+2.19}$ ) is from the resonant tunnelings of three orbitals:  $d_{xz}(d_{yz})$  and  $d_{z^2}$ . These situations only correspond to three energy regions with different PDOS characteristics of the frontier orbitals of the Mn ion (Fig. 4(d)).

From the above analyses, one can find that the replacement of the central metal ion in the MPc molecule dramatically changes the characteristics of STS. Different central metal ions have different localized states with strong components of specific  $d$  orbitals near the  $E_F$ , which couple with the complicated electronic states of the Ni(111) tip, to bring different NDR points with different origins of  $d$  orbitals. In a planar square ligand-field ( $D_{4h}$  point group), such as of MPc, the  $d$  orbitals of the central metal atom are split into four groups:  $d_{x^2-y^2}$ ,  $d_{xy}$ ,  $d_{z^2}$  and degenerate  $d_{xz}(d_{yz})$  orbitals, with their eigen-energies decreasing in turn. From CuPc to MnPc (the experimental and theoretical studies for the case of CoPc in Ref. [5] have shown that the resonant channels of the NDR effect are of

$d_{xz}(d_{yz})$  orbitals), the decreasing occupied number of 3d electrons results in the fact that the split 3d orbitals of the central metal atom shift upward relative to the  $E_F$ ,<sup>[6]</sup> so the main resonant channels of the NDR effect change from the highest  $d_{x^2-y^2}$  orbital to the lowest  $d_{xz}(d_{yz})$  orbitals in our simulation, although the spin-splitting makes the situations more complex, especially for the  $d_{xy}$  and  $d_{z^2}$  orbitals. Different from the conventional W tip, the Ni tip has complex frontier orbitals with various 3d-orbitals-dominated states distributed near the  $E_F$ , so the electron resonant tunneling between the adsorbed MPc molecule with different 3d orbitals localized at the central ion and the Ni tip can result in different 3d-orbital-dominated NDR channels. Here, the Ni tip plays a role of 3d orbital detector with the magnetic quantum number-sensitivity by the appearance of NDR effect.

Different variations of the intensities of the NDR peaks at negative and positive biases with enlarged tip-molecule distance in some cases are supposed to be related to different resonant channels at two biases. For example, in the case of NiPc, the NDR effect at negative bias is mainly contributed by the resonant tunneling of  $d_{xz}(d_{yz})$  orbitals and the one at positive bias originates from the  $d_{x^2-y^2}$  orbital. Considering different spatial extensions of these two types of orbitals in the  $z$ -direction, one can deduce that the normalization based on the setting point at  $-1.0$  V cannot take effect at positive bias. However, in the case of CuPc, the main NDR peaks have similar variations with the enlarged tip-molecule distance because of the same resonant channels from the  $d_{x^2-y^2}$  orbital. It is also noticed that in the case of MnPc, the NDR  $Mn^{+0.47}$  and  $Mn^{+1.31}$  become more obvious at some tip-molecule distances, suggesting that the electron tunneling of the  $d_{x^2-y^2}$  orbitals becomes dominant in the resonant channels compared to those of the  $d_{xz}(d_{yz})$  orbitals in these situations.

Besides the NDR phenomena, one can observe that when the Ni(111) tip is used, the STS of adsorbed CuPc and MnPc present rectifying effects in some voltage ranges (Fig. 2), although they are not strong enough, such as a ratio of about 4 to 6 in the case of CuPc, and a ratio of about 3 in the case of MnPc. This effect can be ascribed to the asymmetrical PDOS of the Ni(111) tip, i.e. stronger PDOS of various  $d$  orbitals below the  $E_F$  than those above the  $E_F$  (Fig. 4(e)), and comparatively symmetrical PDOS of  $d$  orbitals in the adsorbed molecule dominating the transport channel, such as  $d_{x^2-y^2}$  in the case of CuPc (Fig. 4(a)). For the case of MnPc, a strong transport channel related to the  $d_{x^2-y^2}$  orbital just above the

$E_F$  of the Mn ion in the adsorbed MnPc dominates at lower voltage with positive polarity, which enhances the difference between the currents at two polarities originally aroused by the  $d_{xz}(d_{yz})$  orbitals. These mechanisms may be instructive to the future design and application of rectifying device at nano-scale.

In summary, we have carried out a detailed study on the STS of MPc ( $M = Mn, Fe, Ni, \text{ and } Cu$ ) adsorbed on a Au(111) surface when a Ni(111) STM tip is positioned upon the central ion. The simulation results show that various NDR phenomena appear in this experimental configuration, due to the mechanism of local 3d orbital symmetry matching between the central metal ion in the adsorbed MPc molecule and Ni tip. With the decreasing 3d electrons, the energies of the split 3d orbitals of the central ion shift upward, which makes the main resonant channels of NDR effect change from the  $d_{x^2-y^2}$  orbital in the case of CuPc to the  $d_{xz}(d_{yz})$  orbitals in the case of MnPc. Different dependences of intensities of the NDR peaks at two bias polarities on the tip-molecule distance in some cases are related to bias-dependent resonant channels. Lastly, the weak rectifying effects occurring in some cases are ascribed to the asymmetrical PDOS of the Ni(111) tip and comparatively symmetrical PDOS of  $d$  orbitals in the adsorbed molecule dominating the transport channel.

## References

- [1] Tu X W, Mikaelian G and Ho W 2008 *Phys. Rev. Lett.* **100** 126807
- [2] Zhao J, Zeng C G, Cheng C, Wang K D, Wang G W, Yang J L, Hou J G and Zhu Q S 2005 *Phys. Rev. Lett.* **95** 045502
- [3] Hahn J R, Lee H J and Ho W 2000 *Phys. Rev. Lett.* **85** 1914
- [4] Bartels L, Meyer G and Rieder K H 1997 *Appl. Phys. Lett.* **71** 213
- [5] Chen L, Hu Z P, Zhao A D, Wang B, Luo Y, Yang J L and Hou J G 2007 *Phys. Rev. Lett.* **99** 146803
- [6] Liao M S and Scheiner S 2001 *J. Chem. Phys.* **114** 9780
- [7] Lu X and Hipps K W 1997 *J. Phys. Chem. B* **101** 5391
- [8] Gao L, Ji W, Hu Y B, Cheng Z H, Deng Z T, Liu Q, Jiang N, Lin X, Guo W, Du S X, Hofer W A, Xie X C and Gao H J 2007 *Phys. Rev. Lett.* **99** 106402
- [9] Hu Z P, Chen L, Zhao A D, Li Z Y, Wang B, Yang J L and Hou J G 2008 *J. Phys. Chem. C* **112** 15603
- [10] Li Z Y, Li B, Yang J L and Hou J G 2010 *Acc. Chem. Res.* **43** 954
- [11] Zhao A D, Li Q X, Chen L, Xiang H J, Wang W H, Pan S, Wang B, Xiao X D, Yang J L, Hou J G and Zhu Q S 2005 *Science* **309** 1542
- [12] Delley B 2000 *J. Chem. Phys.* **113** 7756
- [13] Vosko S J, Wilk L and Nusair M 1980 *Can. J. Phys.* **58** 1200
- [14] Chen C J 1993 *Introduction to Scanning Tunneling Microscopy* (Oxford: Oxford University)